Supplementary Information

A universal approach for optimizing charge extraction in electron transporting layer-free organic solar cells via Lewis base doping

Rong Wang [a], Boxin Wang [b], Ao Yin [b], Jianqiu Wang [a], Xuning Zhang [a], Xuanye Leng [b], Dongyang Zhang [a], Shuo Yang [b], Zhong Zheng [b], Donghui Wei [c], Xiaobo Sun [a], Huiqiong Zhou [b], Yuan Zhang*[a]

Determination of charge carrier density in solar cells under illumination

To determine the carrier density N_d, impedance spectroscopy and photovoltaic *J-V* characterization were performed on the solar cell under various light intensities (P_{light}). The chemical capacitance *C* and recombination resistance at different P_{light} were extracted based on equivalent model. N_d was determined by integrating *C* over voltage (from dark to V_{oc}) according to the equation,

$$Nd = \frac{1}{qAd}\int_{dark}^{Voc} C(V)dV$$

where *q* is the elementary charge, *A* is the device area and *d* is the film thickness of active layer.

Table S1. Solar cell parameters of studied OSCs with different TXABr dopants.

Doping conditions	V_{oc} (V)	J_{sc} (mA/cm²)	FF (%)	PCE (%)
PBDBT-2F:IT-4F	0.75	20.87	61.08	9.56
w/TMABr	0.82	20.58	66.17	11.16
w/TPABr	0.84	20.74	71.14	12.39
w/TAABr	0.86	20.86	73.50	13.18
w/THABr	0.85	20.90	54.32	9.64
PBDB-T:ITIC	0.72	14.78	62.31	6.34
w/TMABr	0.82	15.73	64.16	8.28
w/TPABr	0.86	16.33	65.19	9.16
w/TAABr	0.88	16.62	70.64	10.33
w/THABr	0.88	15.67	55.41	7.64
PBDB-T:IT-M	0.72	15.42	66.29	8.79
w/TMABr	0.82	16.04	67.59	9.76
w/TPABr	0.86	16.59	71.12	10.62
w/TAABr	0.88	16.92	72.10	11.22
w/THABr	0.88	14.81	52.75	7.18
PBDB-T:ITCC	0.74	12.87	58.78	5.97
w/TMABr	0.90	13.14	60.20	7.12
w/TPABr	0.94	13.73	63.54	8.21
w/TAABr	0.96	13.92	66.95	8.95
w/THABr	0.96	13.23	58.23	7.40
PBDBT-2F:Y6	0.72	24.86	55.97	10.02
w/TMABr	0.82	23.73	70.05	13.63
w/TPABr	0.82	24.52	72.23	14.52
w/TAABr	0.82	24.50	74.92	15.05
w/THABr	0.82	25.42	73.60	15.34
PTB7-Th:$PC_{71}BM$	0.70	16.27	57.59	6.56
w/TMABr	0.80	16.39	66.36	8.70
w/TPABr	0.80	16.20	66.27	8.59
w/TAABr	0.80	16.21	64.49	8.36
w/THABr	0.80	16.19	62.45	8.09

Table S2. Chain length of alkyls and diameter of dopants

Dopants	Chain length of alkyls (Å)	Diameter of dopants (Å)
TMABr	1.707	4.048
TPABr	3.909	6.598
TAABr	5.738	7.088
THABr	7.552	8.873

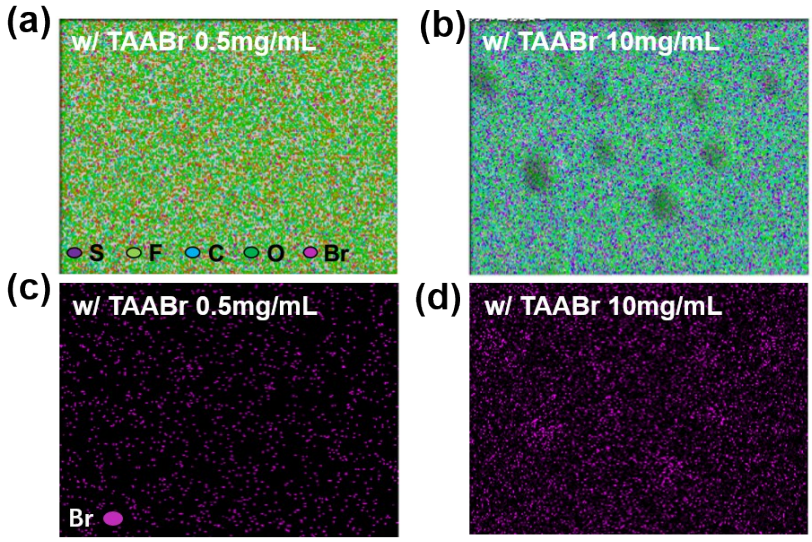

Fig S1. (a), (b) Elemental mapping of carbon and heteroatoms in PBDBT-2F:IT-4F blend films doped with TAABr at low and high concentrations obtained by EDX measurements. (c), (d) EDX mapping of Br distribution in TAABr-doped PBDBT-2F:IT-4F blend films at low and high concentrations.

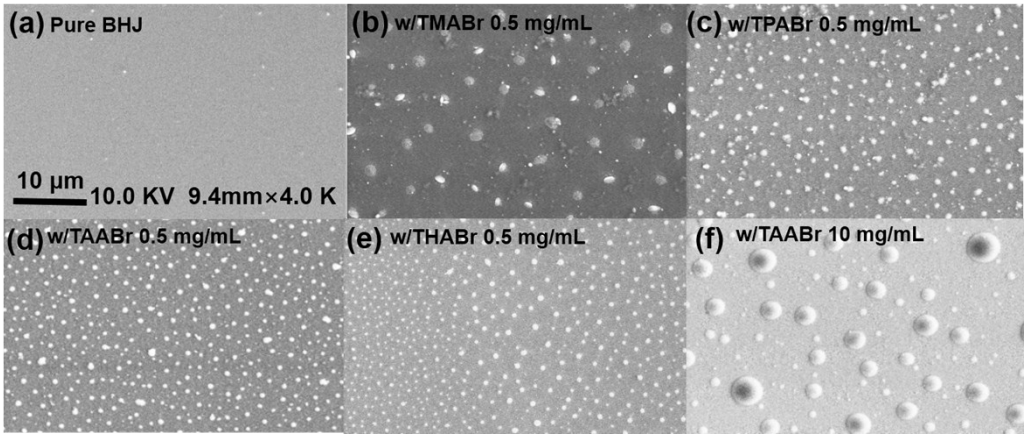

Fig. S2. Top-view SEM images of PBDBT-2F:IT-4F blend films doped with various dopants.

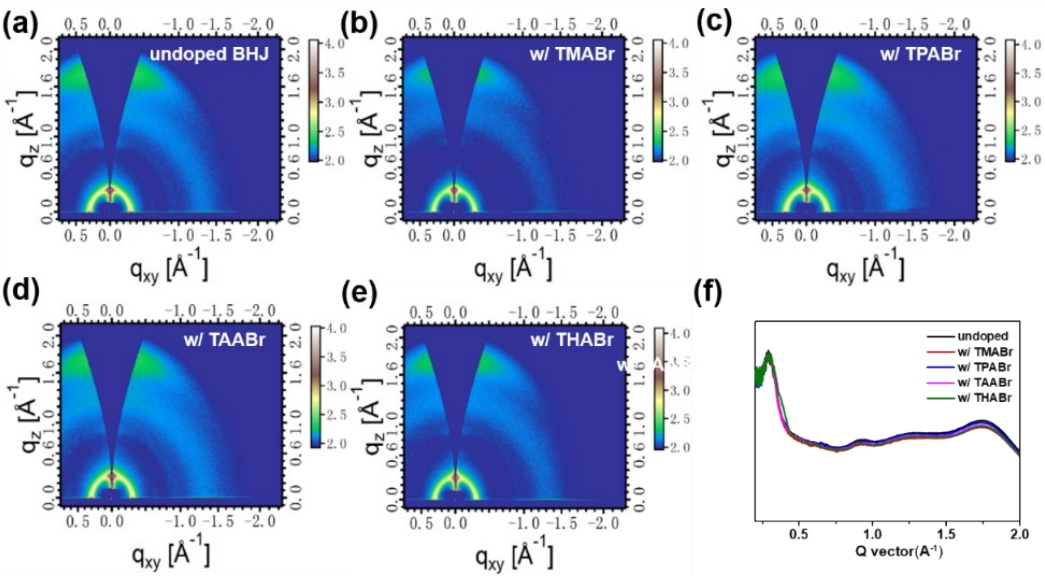

Fig. S3. 2D GIWAXS patterns of various BHJ films of (a) undoped BHJ, (b) BHJ/TMABr, (c) BHJ/TPABr, (d) BHJ/TAABr, and (e) BHJ/THABr. (f) Line-cut curves of 2D GIWAXS of various PBDBT-2F:IT-4F BHJ films along out-plane orientation.

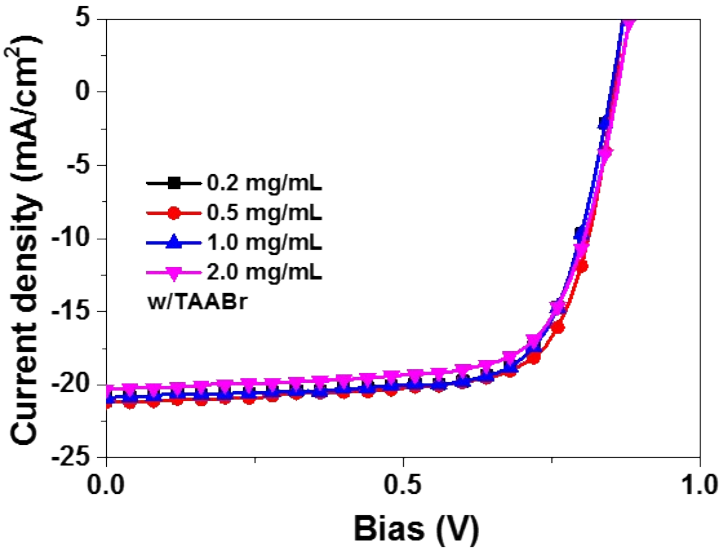

Fig. S4. *J-V* characteristics of PBDBT-2F:IT-4F solar cells under AM 1.5 g irradiation deposited with different concentrations of dopants (in methanol).

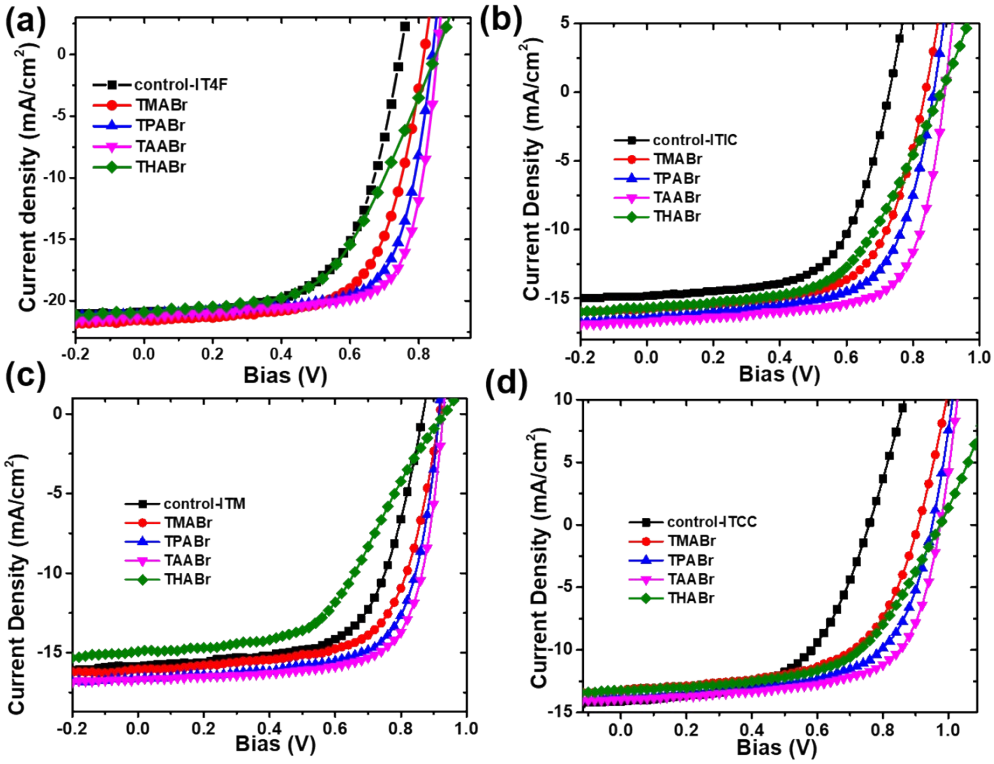

Fig S5. (a)-(d) Current density versus voltage characteristics of PBDBT-2F:IT-4F, PBDB-T:ITIC, PBDB-T:ITM and PBDB-T:ITCC solar cells doped with various dopants (concentration: 0.5 mg/mL) under AM 1.5 G solar irradiation (100 mW/cm^2).

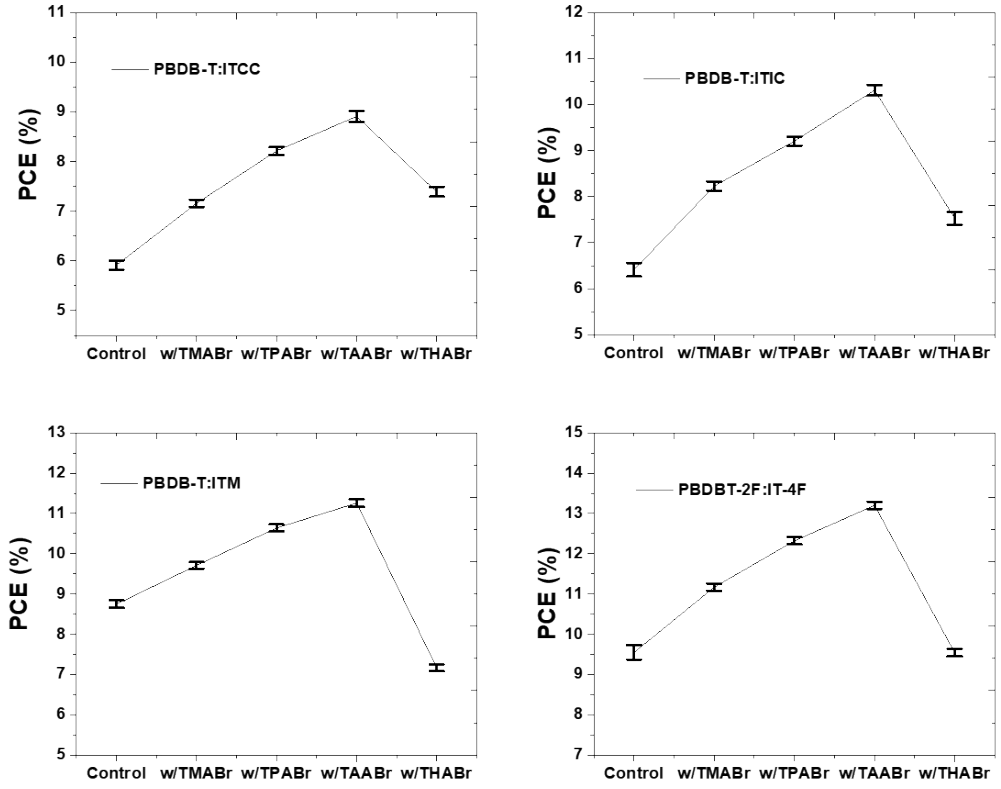

Fig S6. (a)-(d) PCEs together with error bars of PBDB-T:ITCC, PBDB-T:ITIC, PBDB-T:ITM and PBDBT-2F:IT-4F solar cells doped with various dopants (concentration: 0.5 mg/mL) under AM 1.5 G solar irradiation (100 mW/cm^2). In each doping conditions, the efficiency is averaged based on 8 devices.

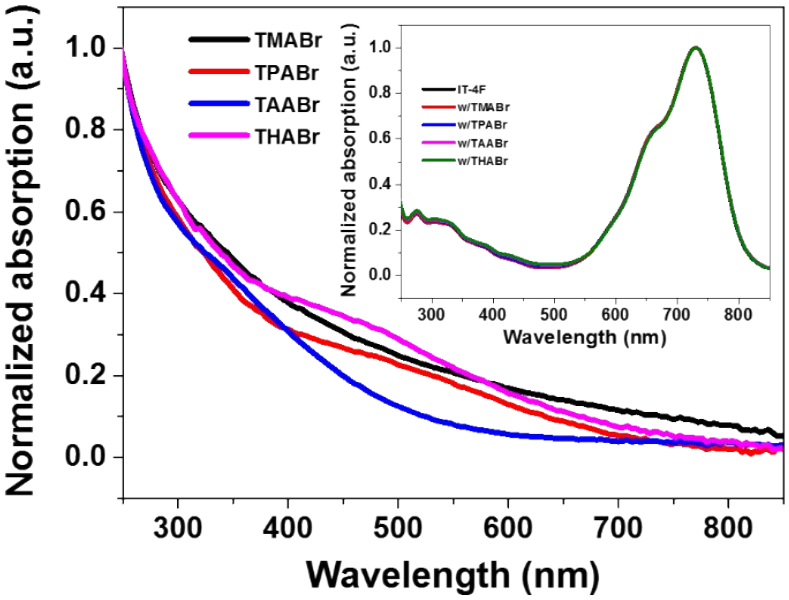

Fig S7. Absorbance of pure dopants in solution together and thin films of pristine IT-4F acceptor and interfacially doped IT-4F (doping concentration is 0.5mg/mL in methanol).

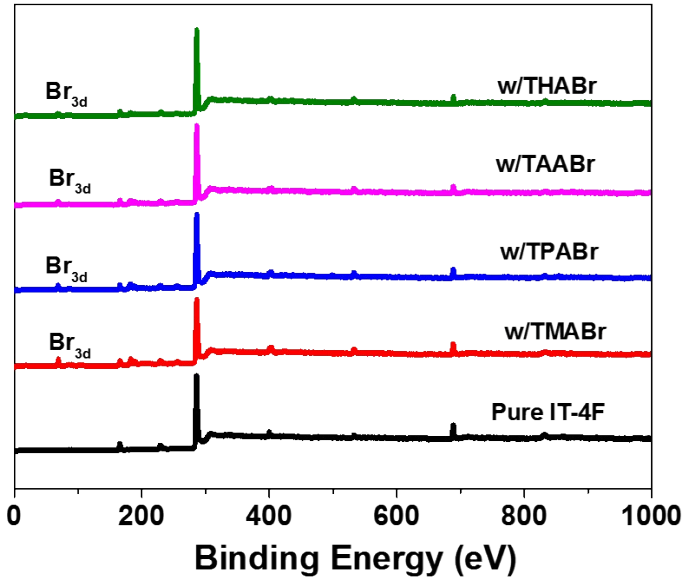

Fig. S8. XPS survey spectra of pristine IT-4F and IT-4F doped with various TXABr dopants.

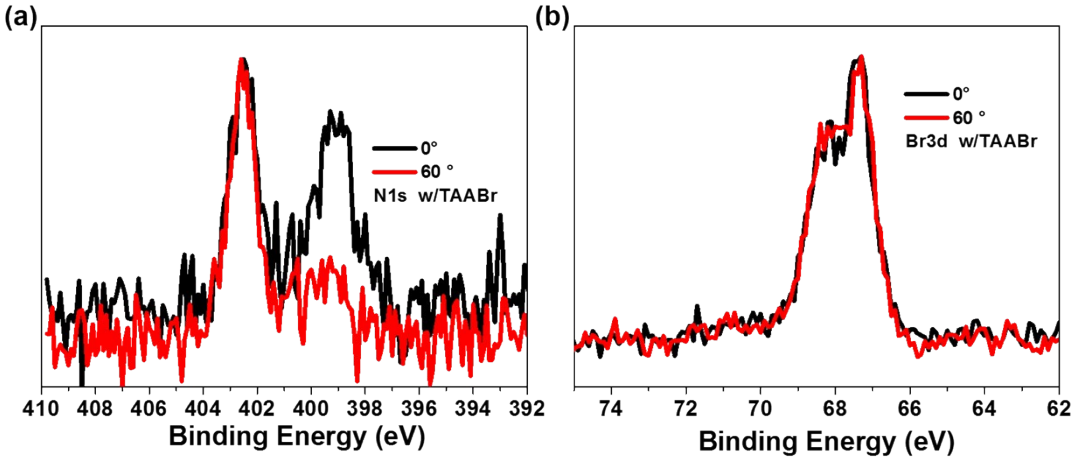

Fig. S9. Angular-dependent XPS measured on thin film of IT-4F/TAABr for core level N1s (a) and Br3d (b).

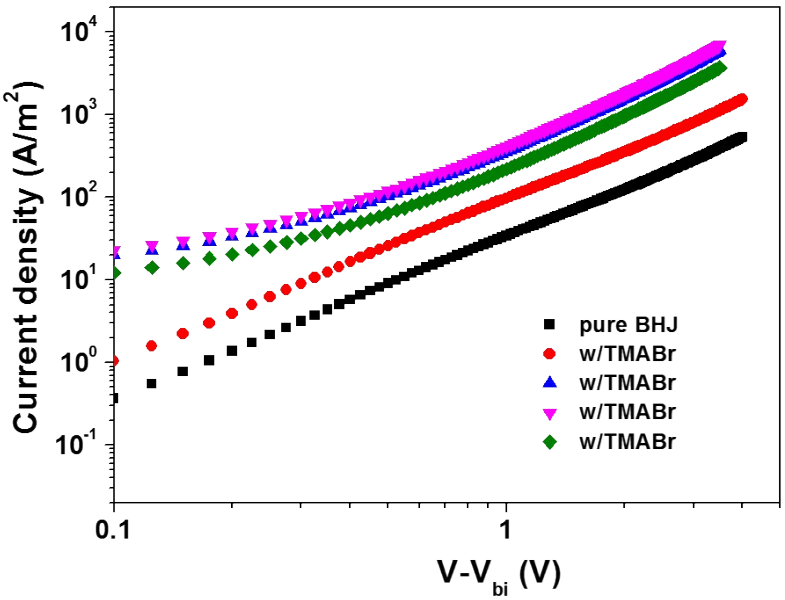

Fig. S10. *J-V* characteristics in dark of single-carrier devices (electron-dominant) based on PBDBT-2F:IT-4F blend films doped with various TXABr dopants.

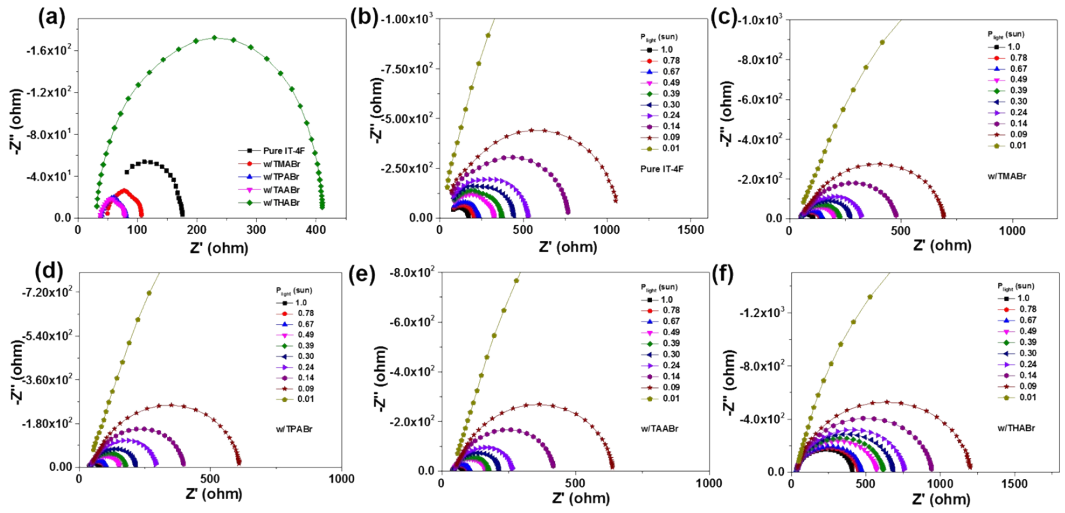

Fig. S11. (a) Nyquist plots of impedance spectroscopy (IS) of various PBDBT-2F:IT-4F solar cells under 100 mW/cm^2 (1 sun) irradiation (short-circuit condition). (b)-(f) Irradiation intensity-dependent Nyquist plots of IS (open-circuit condition) of undoped (b) and doped PBDB-TF:IT-4F solar cells with various dopants of TMABr (c), TPABr (d), TAABr (e), and THABr (f).

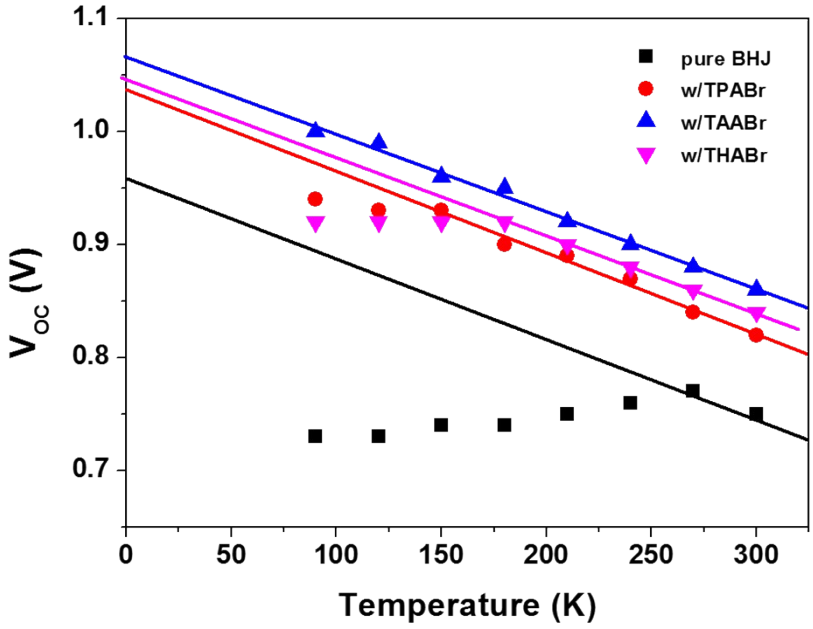

Fig. S12. Temperature-dependent photovoltage measurements under AM 1.5 g irradiation for PBDBT-2F:IT-4F solar cells.

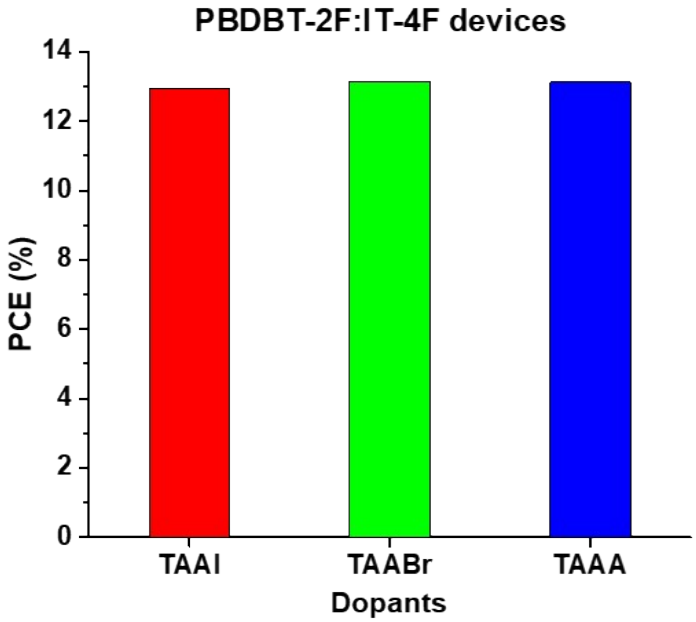

Fig. 13. Efficiencies of PBDBT-2F:IT-4F solar cells without doping and doped with different tetrabutyl ammonium dopants containing different anions of Br^- (TAABr), I^- (TAAI), and AcO^- (TAAA). Chain length of all dopants is pentyl.

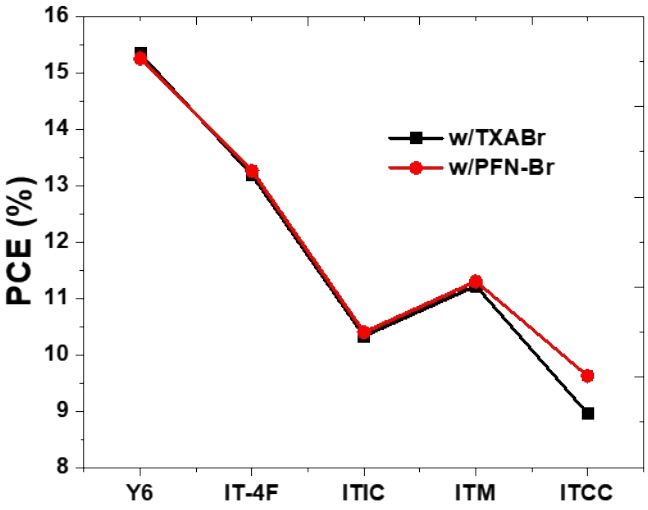

Fig. 14. Comparison of PCEs in various NF-organic solar cells containing the PFN-Br electron transporting layer (ETL) and TXABr-doped devices without using PFN-Br ETLs.